



Research article

UDC 691.3

DOI: 10.34910/MCE.126.4



Input parameters of three-layer steel fiber concrete beams

T.Q.K. Lam 

Mien Tay Construction University, Vinh Long city, Vietnam

 lamthanhquangkhai@gmail.com

Keywords: reinforced concrete, fiber reinforced concrete, stress-strain, numerical simulation, multilayered beam, bending beam

Abstract. Many researchers have shown interest in the study of bending concrete beams. One method involves using multilayer concrete beams with a layer of steel fiber concrete. This technique aims to improve the beams' capability for supporting load and to minimize the occurrence of cracks, particularly in areas subjected to high compressive and tensile stress. The primary goal is to reduce the stress in these beams. An advantage of using three-layer steel fiber reinforced concrete beams is the ability to repair damaged beams by adding another layer of concrete on top or below the existing concrete layer. Modifying the input parameters during the three-layer beam design process significantly impacts the overall effectiveness of the beams. In this study ANSYS simulation and nonlinear material analysis was used. The objective of the study was to investigate the behavior of three-layer bending concrete beams subjected to two concentrated loads. Specifically, the study examined the impact of varying the content of steel fiber in the concrete, as well as the effects of slirrup at the ends of the beams. Furthermore, the study explored the influence of changes in the quantity and size of steel bars in the places of tensile strength, along with the effect of varying the steel fiber concrete layer's thickness. The research results on three-layer beams were used to create diagrams that depicted the relationship between load and vertical displacement, load and stress in the compressive area, and load and stress in the tensile zone. These diagrams also helped to determine the initiation and progression of cracks in three-layer beams, starting from the application of load until the utter damaging of beams. Ultimately, this information allowed to identify the specific load level that had caused the cracking and the damaging of beams.

Citation: Lam, T.Q.K. Input parameters of three-layer steel fiber concrete beams. Magazine of Civil Engineering. 2024. 17(2). Article no. 12604. DOI: 10.34910/MCE.126.4

1. Introduction

In research on new concrete materials, various types of concrete were investigated, such as high-strength concrete, inorganic concrete, organic concrete and steel fiber (SF) reinforced concrete. These materials were added to enhance the bearing capacity of concrete, improve its characteristics and reduce the occurrence of cracks in concrete beams. In order to create multilayer reinforced concrete (RC) beams, the process involves repairing damaged RC beams (RCB) by adding a new layer of concrete either above, below, or both above and below the existing concrete. To successfully repair damaged RCBs, it is crucial to thoroughly examine the input parameters, particularly in the case of three-layer steel fiber RCB. Numerous researchers have used nanosilica in their studies on SFRC. Their aim is to enhance the tensile strength and plasticity of nano concrete containing SFs. Consequently, these researchers have examined the impact of nanosilica on high-performance concrete that incorporates SF [1, 2].

Numerous studies have been conducted on the use of thin multilayer shells to repair damaged shell roofs. These studies have focused on various aspects, such as investigating the formation and development of cracks in the shell through experimental and ANSYS numerical simulation methods. Furthermore, studies have been carried out to establish relationships between load, vertical displacement (VD), and stress when evaluating the thickness of the SF concrete layer (SFCL) in the compressible shell

[3–5]. Numerous studies have been conducted on SF RCBs. These studies have focused on investigating the cracking and stress-strain states of RCB by modifying the SF content in the concrete. For example, different SF contents, such as $\mu=0\%$, $\mu=2\%$, $\mu=4\%$, and so on, have been examined in the studies [6], [7]. Several researchers have conducted studies on delaminated composite beams, focusing on various aspects, such as bending analysis, cracking propagation, and bending of composite beams [8, 9].

Iskhakov and his colleagues conducted a study on multilayer RCBs [10]. They had analyzed beams made of high strength concrete (HSC) in the compression zone and normal strength concrete (NSC) in the tensile zone. The research presented and examined the issues associated with different types of beams. Each layer was prescribed with an appropriate depth. The compatibility conditions between HSC and NSC layers were established. The premise was based on the assumption that the shear deformations on the layer borders in a section had been equal, particularly in the section with maximal depth of compression zone. A rigorous definition of HSC was given for the first time, achieved by careful analysis and comparison of deformability and strength characteristics of different classes of concrete. The application fields of two-layer concrete beams, including specific static schemes and load conditions, was made known. The main disadvantage of HSCs is their low ductility. To overcome this, fibers were incorporated into the HSC layer. Iskhakov's study examined the impact of different fiber volume ratios on structural ductility.

An evaluation was conducted on the strength of reinforced concrete beams made of high-performance concrete and fiber reinforced concrete through a bending test. An evaluation was conducted to assess the efficiency of utilizing steel fiber in bending structures. The significance of calculating the fiber content for such elements, similar to that of reinforcing steel bars for typical RC beams, was highlighted [11–12].

The experimental study [13] focused on two-layer beams made of steel fibered high strength concrete (SFHSC) in the compression zone and NSC in the tensile zone. Calculating the fiber content for two-layer beams was essential corresponding to the required ductility level of an RC element. This research was focused on testing full scale two-layer beam. The purpose of this work was to show the efficiency of two-layer bending element during the whole loading process, including collapse, and to experimentally verify the data related to interaction of concrete layers in two-layer beams. After the NSC layer was hardened, the SFHSC layer was cast to examine the influence of separate casting technology, which is more convenient for two-layer beam production in real construction.

The same authors performed tests on models of full-scale statically determinate two-layer beams in another study [14]. These beams were also constructed using SFHSC in the compression zone and NSC in the tensile zone. The current study represented the next phase of these investigations, focused on testing a continuous two-span two-layer beam with an optimal steel/fiber ratio, similar to the previous phases. The objective of this study was to examine the behavior of the continuous two-layer beam in both the span and above the middle support. Additionally it was investigated how the continuous two-layer beam responded to both positive and negative bending moments. This study was part of a series of investigation on two-layer beams [15]. In this series, a two-layer beam concept was designed, SFHSC was tested, as were the materials for simple supported and continuous two-span two-layer beams. The focus of the current research was testing full-scale prestressed simple supported two-layer beams. The objective of this study was to examine the behavior of prestressed two-layer beams at four-point bending and to compare it with the behavior of nonprestressed beams. No de-bonding has been observed between the SFHSC and the NSC layers in the tested beams up to the ultimate limit state. This indicated that there had been a proper interaction between the layers. The results suggested that further investigation of prestressed two-layer beam had been recommended for full-scale RC elements with longer spans (9–12 m). This research also highlighted the potential practical application of prestressed two-layer beam as effective and economical bending solution.

In structural analysis, the concept of concrete stiffness is important since it indicates the performance of beam elements in resisting deflection due to the working loads. In the study [16], the behavior of the graded concrete beam was continually examined. The bending moment-curvature relationship of the graded concrete beam was performed numerically to understand the level of ductility and the failure mode in relation to the conventional beam. A singly reinforced graded concrete beam was modelled using a non-linear simulation program Strand7. The result of the analysis was then evaluated in accordance with the Eurocode. The graded concrete beam "was expected to show a reliable behavior of bending moment – curvature so that it was possible for advanced application as structural element".

Numerical studies of these structures' stress-strain state under different types of loading are required in order to efficiently build multilayer structures out of concrete with different physico-mechanical characteristics. In the article [17] was analyzed the effect of concrete and cross section materials for the stress-strain state of three-layer RC with light weight concrete in the internal layer and heavy concrete in the external layers. The study showed that differences in the external layer's height and material had a substantial impact on the stress and deformation state of the three-layer beam under the different loads.

Rational specifications for the geometric cross section and materials used in various structural solutions for multilayer RC constructions were determined through scientific results. The research on three-layer beams [18] investigated the impact of geometrical parameters of the cross section, as well as the strength and deformability of the materials used in the stress-strain state and finite element analysis. This study focused specifically on the effect of these factors on the three-layer RCB with composite reinforcement. In addition, the study [19] examined the design parameters of RCB that impacted their bearing capacity. A separate study on multilayer RCB are presented in the References section of this article [20–26].

Further research should be conducted on multilayer beams, with a specific focus on three-layer SFRCB. These beams consist of upper and lower layers made of SF concrete, while the middle layer is made of normal concrete. The inclusion of concrete SF layers in the tensile zone and compressive area of the beams has the potential to improve their bearing capacity and minimize cracks in the bending beams. Therefore, it is important to explore and expand upon the study of these multilayer beams. In this paper, the author used ANSYS numerical simulations to examine the input parameters involved in the design of three-layer SFRCBs. These parameters have an impact on the bearing capacity of the beams, as well as on the formation and progression of cracks. The study focused specifically on factors such as the content of SF in concrete, the spacing of the shear steel stirrups at the ends of the beams, the number of tensile steel bars, and the thickness of the concrete layer of SF. The author constructed a diagram of how cracks in three-layer beams started and spread. The relationships between load and tensile stress (L-TS), load and compressive stress (L-CS), and load and vertical displacement (L-VD) are shown in the diagram. The author worked with ANSYS software to create simulation of RCB work, which allowed to calculate the stress at which the beam began to fail and become damaged.

2. Materials and Methods

2.1. Design Model of Beams

The research involved studying a three-layer beam made of steel fiber reinforced concrete (SFRC). The beam had a layer of SFRC on both the upper and lower layers, while the middle layer was made of normal concrete (NC). The dimensions of the beam were 15×30×220 cm. The SFCL was of grade B30, while the NC layer at the center of the beam was of grade B20.

Figure 1 shows the design of the three-layer RCB model.

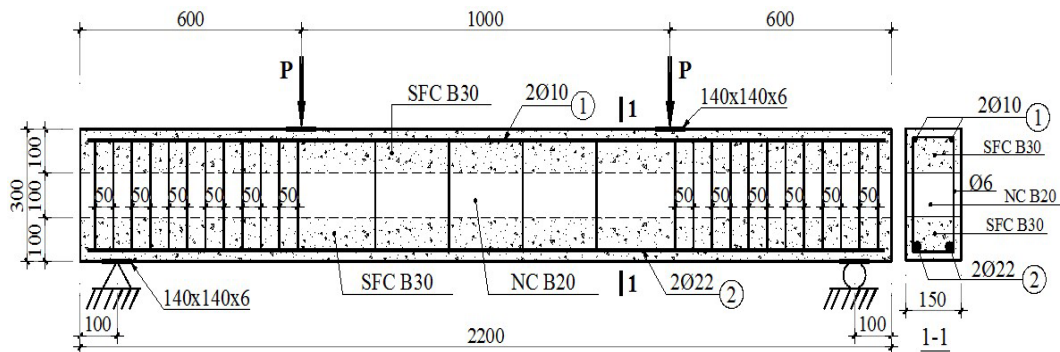


Figure 1. The design of the three-layer reinforced concrete beam model.

2.2. Finite element model for the three-layer reinforced concrete beams

Choosing the right model of SF dispersed in concrete is a crucial decision. The following models were used: smeared model, embedded model, and discrete model. The smeared model was used to represent the dispersion of SFs in concrete in this study.

Currently, there are two main models that are used to represent cracks in concrete: discrete model and smeared model. In this study, the focus was on examining the relationship between load and displacement. We were primarily interested in understanding this behavior and its correlation, without placing significant emphasis on factors such as crack shape or local stress. Therefore, the smeared model had been chosen to study cracks in concrete.

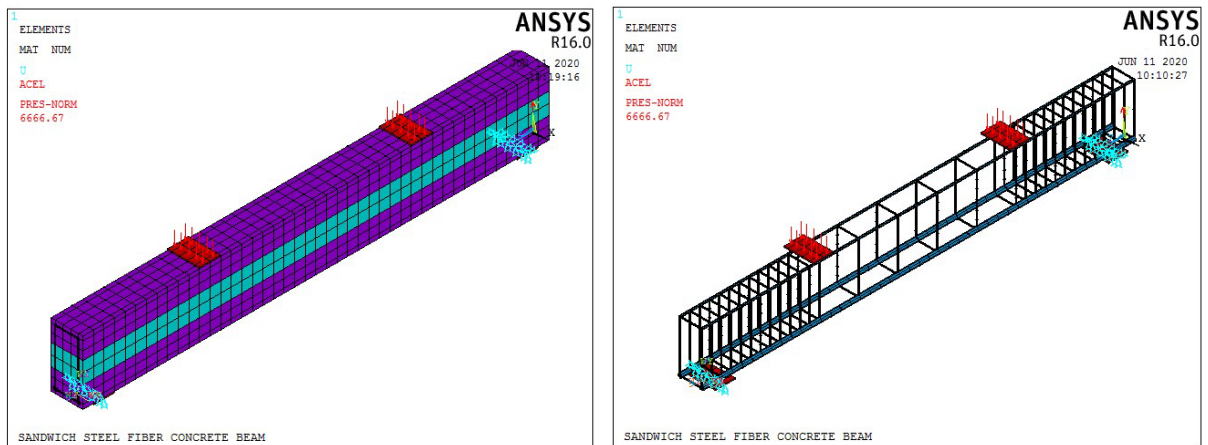
The modelling of reinforcement bars can be achieved by using the BEAM188 element, which consists of two nodes. Finite element modelling in beams is a technique used to analyze the structural behavior of beams. The SOLID65 element is a specialized simulation element that can accurately model concrete materials. It is capable of simulating the behavior of reinforcement in concrete, including phenomena such

as cracking and compression. Additionally, it allows to define nonlinear material properties. This element is three-dimensional and consists of eight buttons.

The mesh shapes in ANSYS were divided by 3D blocks because of the simple beam structure. Additionally, the element size was optimized for better performance. To input the parameters for the SOLID65 concrete element in ANSYS, we needed to specify eight essential parameters:

- 1) the shear force transmission coefficient when the crack is opened,
- 2) the shear force transmission coefficient when the crack is closed,
- 3) the cracking stress in tension,
- 4) the compressive stress,
- 5) the reduction coefficient for weakening due to cracking in tension,
- 6) the modulus,
- 7) Poisson's coefficient,
- 8) the stress-strain relationship.

Figure 2 shows the three-layer beam model in ANSYS.



a) three-layer beam model

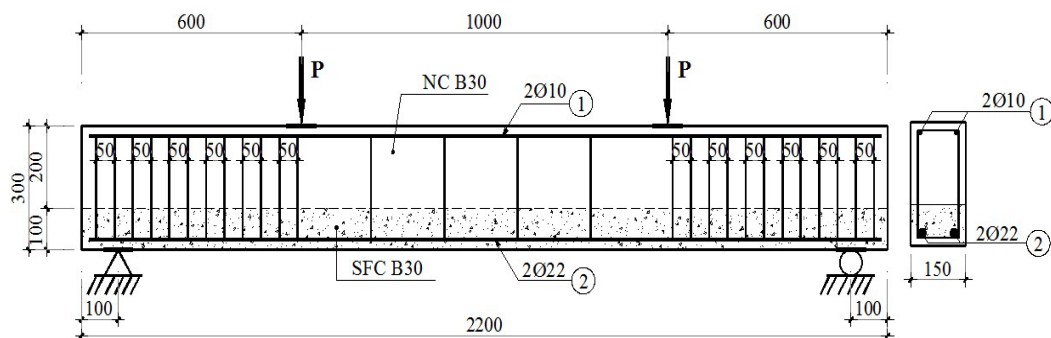
b) steel bar model, borders conditions and loads

Figure 2. Model of three-layer beams.

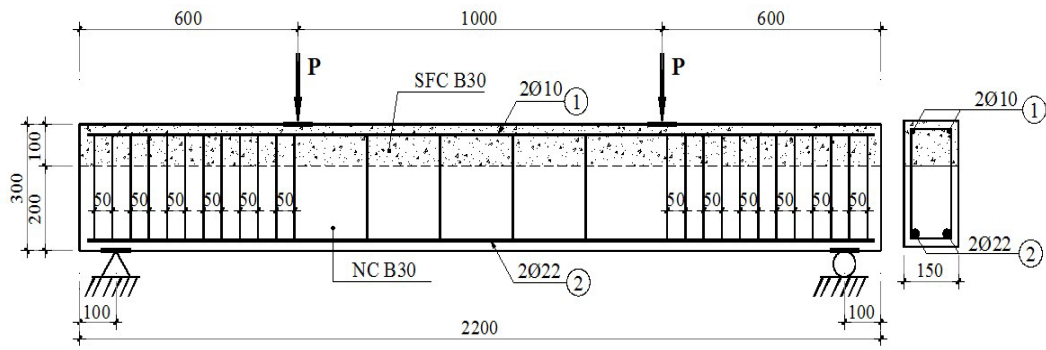
3. Results and Discussion

The author compared the accuracy of the two-layer beam testing method with the three-layer beam (TLB) model constructed in ANSYS. The two-layer beam was constructed to be the same size as the TLB, since there were no experimental results available for the TLBs to serve as a basis for the beam survey.

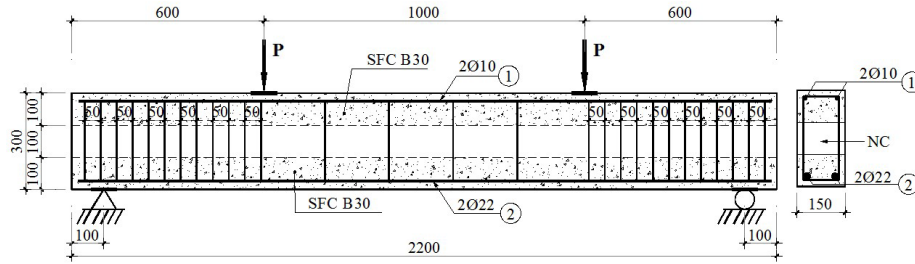
The design model in Figure 3 shows two-layer and three-layer RCBs.



a) The steel fiber layer is located at the bottom.



b) The steel fiber layer is located on top.



c) A three-layer SFRF beam.

Figure 3. Model of two-layer and three-layer reinforced concrete beams

Figure 4 shows the process of concreting beams in layers.



Figure 4. Concreting beams in layers.

Figure 5 shows the test beams.



Figure 5. Test beams on the experimental pedestal.

Figure 6 shows the measuring devices.

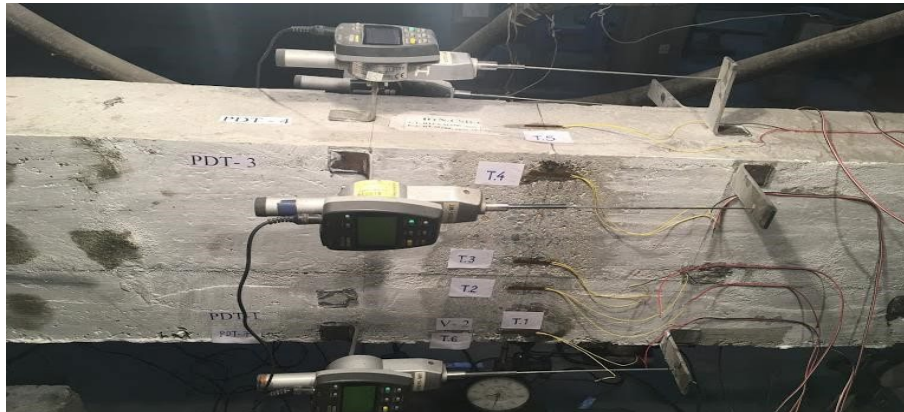


Figure 6. The beams had measuring devices on them.

The formation and development of cracks are shown in Figure 7.



Figure 7. Formation and development of cracks in test beams.

The L-VD relationship in the middle of RCB is shown in Figure 8.

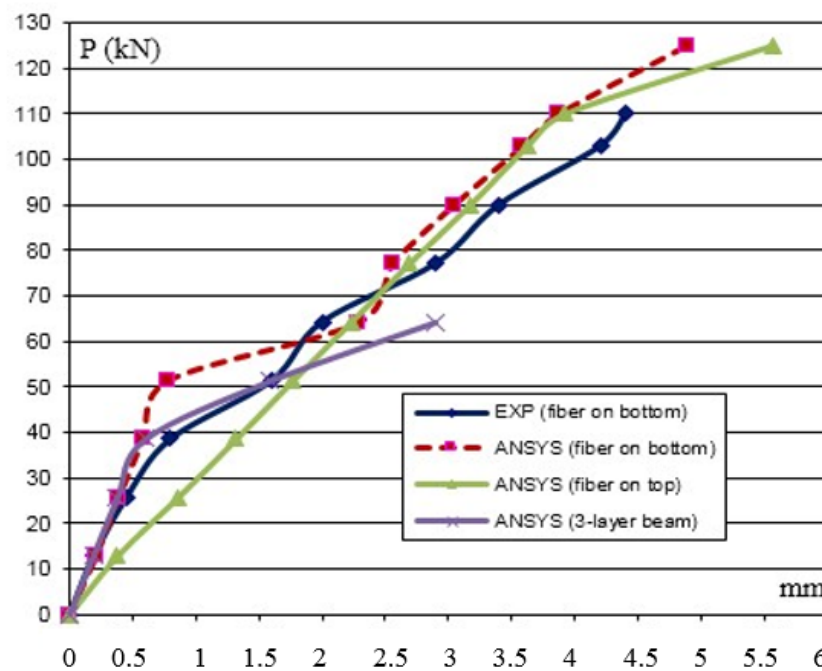
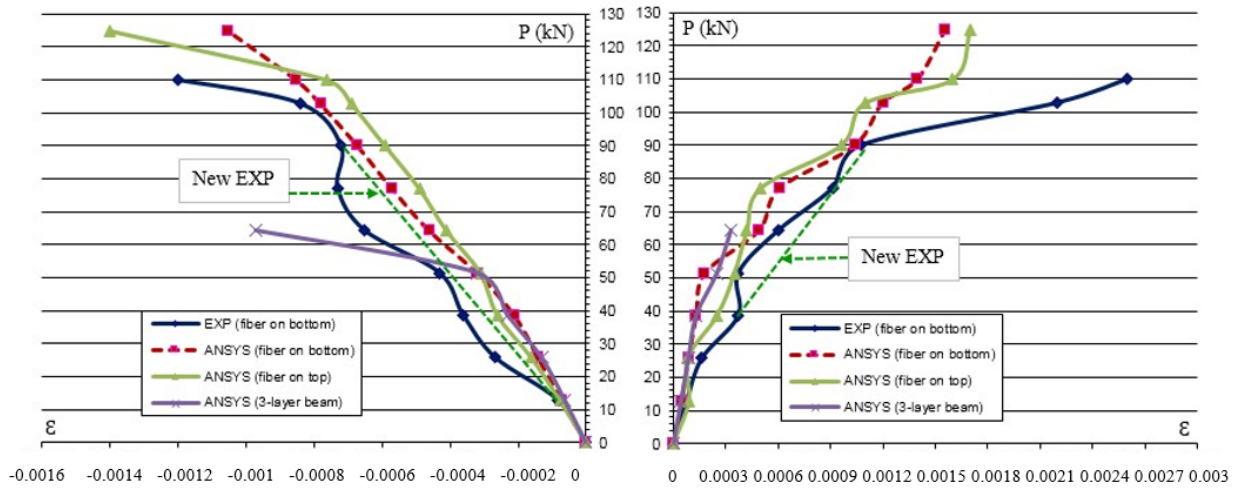


Figure 8. vertical displacement at the middle of reinforced concrete beams

The relationship between load and compressive deformation (L-CD), as well as the relationship between load and tensile deformation in the middle of RCB, are shown in Figure 9.



a) Load - compressive deformation relationship b) Load - tensile deformation relationship

Figure 9. Load - deformation relationships of reinforced concrete beams.

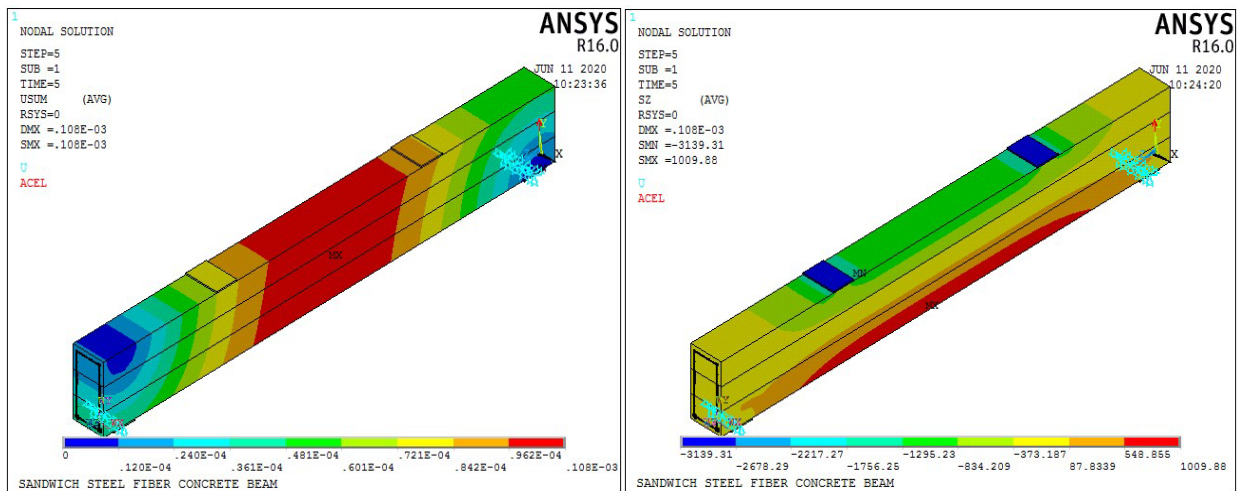
Comment: After comparing the results of test beams and simulations in ANSYS for the survey, it was proven that the program had been designed correctly. It can be used effectively to change input parameters. The input parameters that affect the stress-strain state and VD in SFRC beam are following:

- the content of SF in concrete,
- the spacing of the shear steel stirrups at the ends of RCB,
- the number of TS bars,
- the diameter of TS bars and the thickness of the SF concrete layer.

3.1. Investigation of the effects of changes in SF content on the properties of concrete

The concrete SF content was adjusted to 2 % and 4 % from its initial 0 %. Stirrups, with a diameter of $\phi 6a50$, were placed at the ends of the beam. In the middle of the beam stirrups with a diameter of $\phi 6a200$ were used. TS bars with a diameter of $2\phi 22$ were used, while compression steel bars with a diameter of $2\phi 10$ were used. The thickness of the SF concrete layers, both at the bottom and at the top, was set at $H1 = H2 = 10$ cm. Furthermore, a NC layer with a thickness of $H3 = 10$ cm was placed in the middle of the beam. It is important to note that the numerical simulation analysis in ANSYS considered non-linear materials.

Figure 10 shows VD and the stress color spectrum.



a) Color spectrum of vertical displacement

b) Color spectrum of stresses

Figure 10. Color spectrum of VD and stresses values on the beam.

Comment: In Figure 10a the middle of the beam has the biggest VD; as it gets closer to the supports, the value decreases. Tensile stress is centered on the bottom of the beam, with the maximum value occurring in the middle of the beam, as indicated by the color spectrum of the prestresses in Figure 10b. On the other hand, the compressive stress is located in the upper part of a beam and is affected by the force applied by two concentrated forces. This demonstrates that the beam's actual operating conditions are accurately simulated by ANSYS.

The beams begin to crack when there is a change in the SF content in the concrete, as shown in Figure 11.

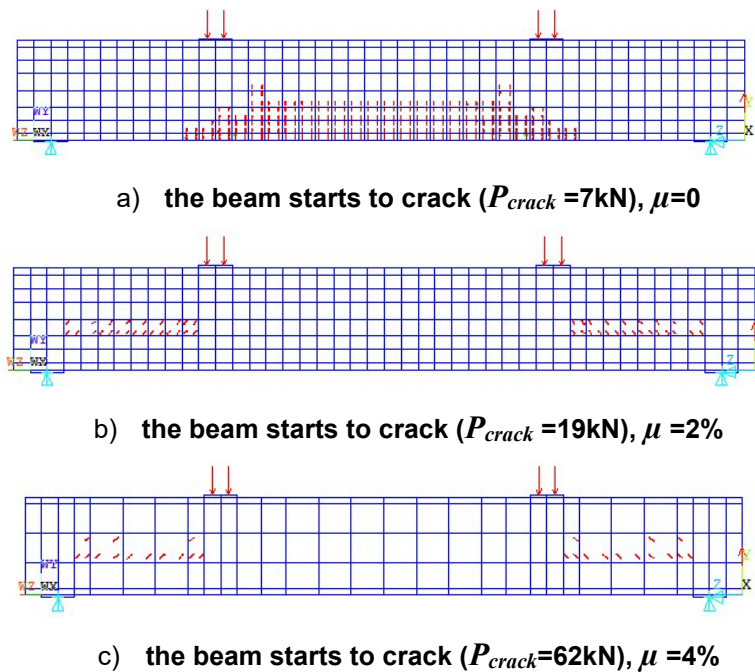
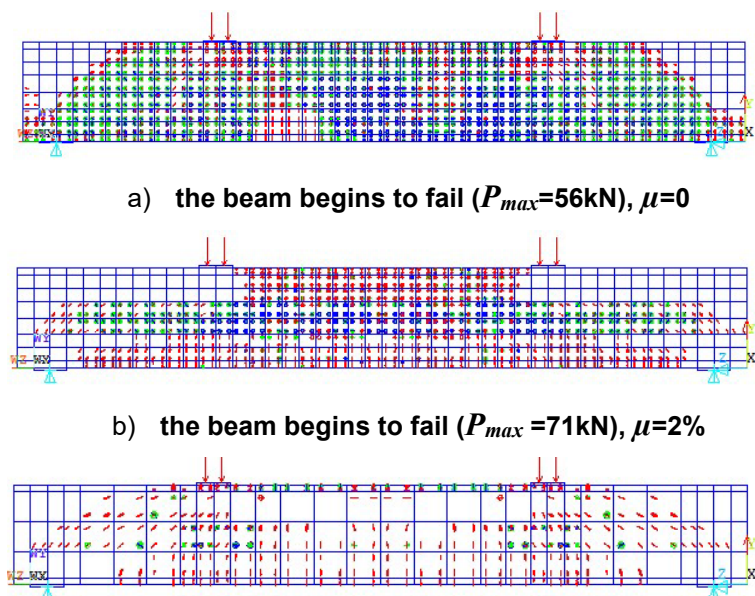


Figure 11. The beginning of beam cracking in the ANSYS.

Comment: In Figure 11a the three layers consist of NC. As a result, cracks initially appear in the part with the highest tensile stress, which is located at the bottom of the beam. These cracks then progress towards the compressive area. In Figures 11b and 11c the lower layer consists of SFRC, which has a higher intensity compared to the NC layer in the middle. As a result, the cracks initially appear in the middle layer of the beam. By increasing the SF content in concrete from 2 % to 4 %, load-induced cracking increased from 19kN to 62kN. This happens because the concrete layer in the tensile zone consists of SF concrete, resulting in fewer cracks and a higher bearing capacity of the beam.

The beams begin to fail when there is a change in the SF content in the concrete, as shown in Figure 12.



c) the beam begins to fail ($P_{max}=122\text{kN}$), $\mu=4\%$

Figure 12. Beginning of beam failure in ANSYS.

Comment: In Figure 12a it was observed that RCB without any SF content began to show signs of damage at a load level of 56kN. Cracks were observed in the RCB. However, when the SF content was increased to 2 %, the destructive load of the beams also increased to 71kN. Furthermore, the presence of SFs resulted in a decrease in the number of cracks compared to beams without any SF content. By increasing the content of SFs to 4 %, the bearing capacity of the beam is further enhanced, reaching 122kN. Furthermore, the presence of SFs in concrete has significantly reduced the appearance of cracks in the beam. This demonstrates that the inclusion of SFs not only minimizes cracks, but also increases the beam's ability to withstand force.

The L-CS, L-TS and L-VD relationships are shown in Figure 13.

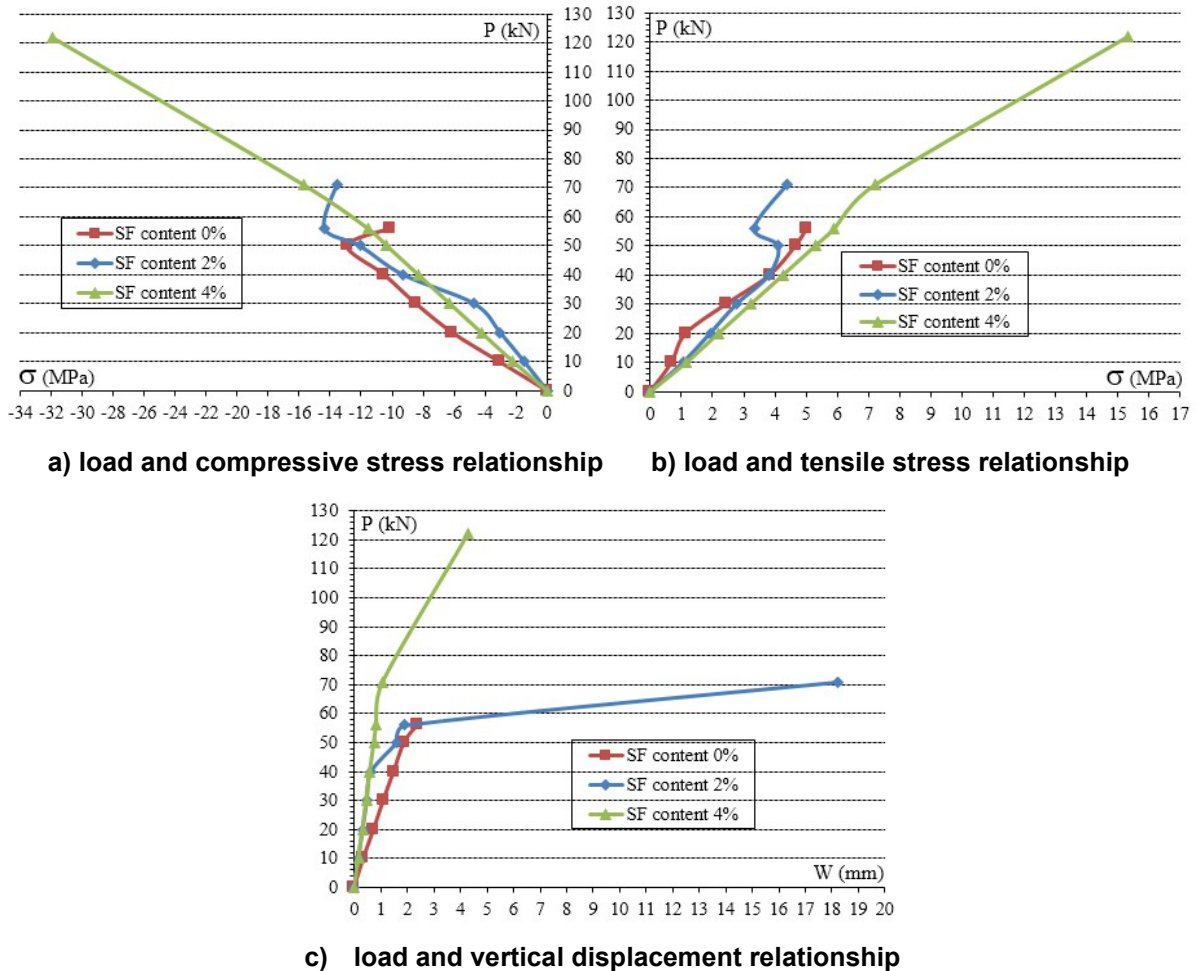


Figure 13. load and compressive stress, load and tensile stress and load and vertical displacement Relationships in the Beam, where SF content refers to the SF content present in concrete.

Comment: In Figure 13a it can be observed that normal RCB with SF content of 0 % shows the minimum compressive strain value. On the other hand, Figure 13b shows that beams with SF content of 4 % have the highest tensile strain. The VD of normal RCB is greater than that of other beams. When concrete contains 0 % and 2 % SFs, VDs are approximately equal under loads ranging from 0 to 56kN. However, once the limit is exceeded, the stress levels show significant variation.

3.2. Investigation of the effects of changes in shear steel stirrup spacing at the ends of the beam

RCB had a SF content of 2 %. The spacing of the stirrups has been changed from $\phi 6a50$ to $\phi 6a100$. TS bar had a diameter of $2\phi 22$, while the compression steel bars had a diameter of $2\phi 10$. The thickness of the SF concrete layers was $H1 = H2 = 10$ cm, and the thickness of the NC layer was $H3 = 10$ cm. The ANSYS numerical simulation analysis considered non-linear materials as shown in Figure 14.

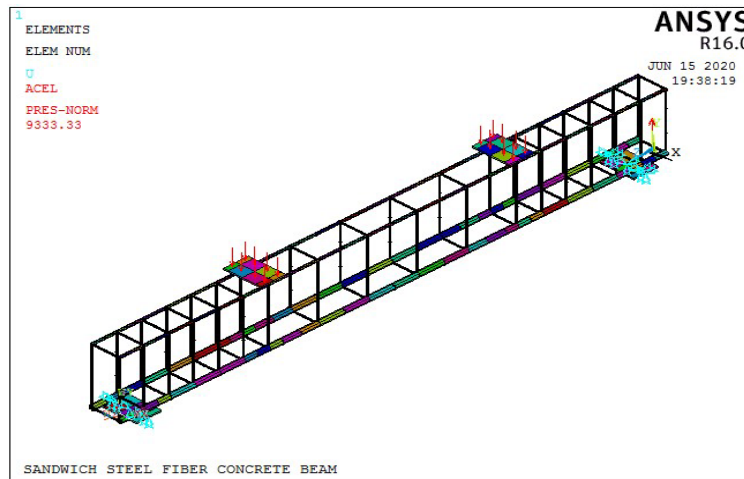


Figure 14. Shear steel stirrup spacings are changed.

The beams began to crack and fail when the stirrups at the ends of the beam had changed, as shown in Figure 15.

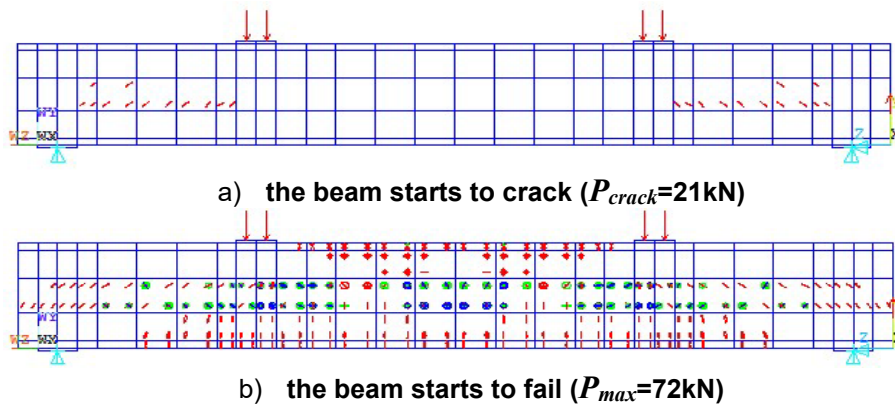
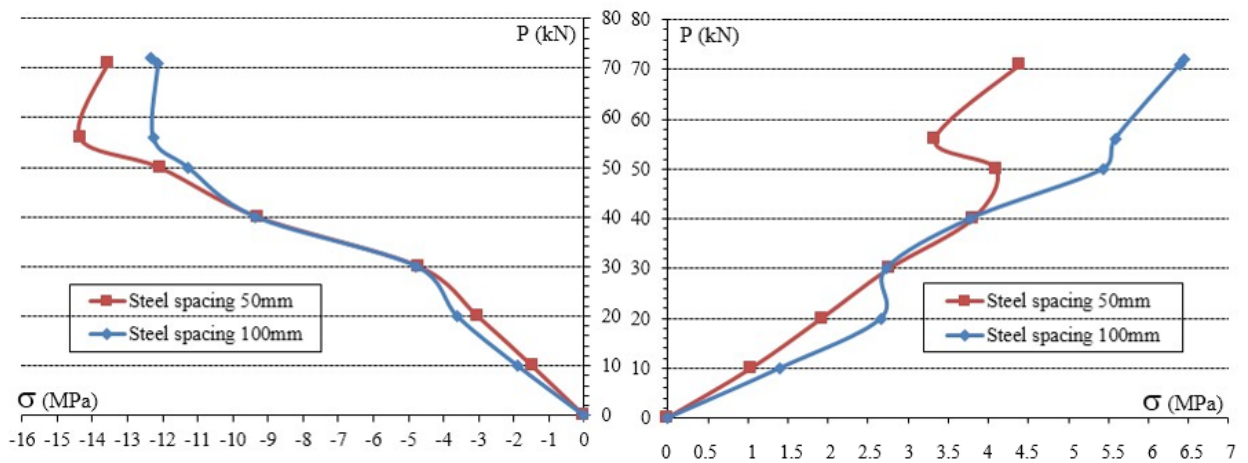


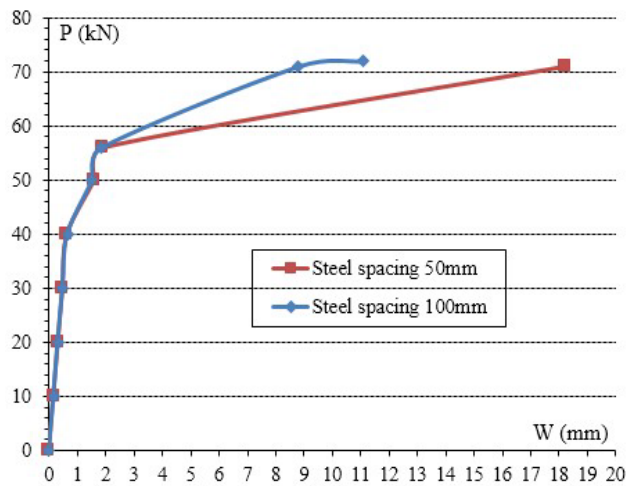
Figure 15. Beams start to crack and fail when shear steel stirrup spacing is changed.

Comment: In Figure 11b the beam shows cracking at a load of 19 kN, when the shear steel stirrup spacing at the ends of the beam is 50 mm. When the shear steel stirrup spacing is increased to 100 mm, the beam experiences cracking at a higher load of 21 kN. Furthermore, the beam begins to show signs of damage when the shear steel stirrup spacing is 50 mm, with a load of 71 kN. Lastly, when the shear steel stirrup spacing is 100 mm, the beam begins to show signs of damage at a load of 72kN. However, the number of cracks in the beams decreased significantly at the shear steel stirrup spacing 100 mm. This is due to the shear steel stirrup spacing being too thick and the steel content in concrete exceeding the allowed content value of steel in concrete.

The L-CS, L-TS and L-VD relationships are shown in Figure 16.



a) load and compressive stress relationship b) load and tensile stress relationship



c) load and vertical displacement relationship

Figure 16. load and compressive stress, load and tensile stress and load and vertical displacement relationships.

Comment: In Figures 16a and 16b, as the load increases from 0 kN to 40 kN, both compressive and tensile stresses experience minimal changes. However, beyond 40 kN, these stress values begin to vary. It should be noted that the steel stirrup spacing is 100 mm, which is smaller compared to the shear steel stirrup spacing of 50 mm. Additionally, the tensile stress in the former is greater than that in the latter. The shear steel stirrups are placed at a spacing of 100 mm, which is reduced to 50 mm in situations where there is VD.

3.3. Investigation of the effects of changes in TS bars number on the beam

The RCB had a SF content of 2 %. The spacing of the stirrups was $\phi 6a100$. TS bars had been changed from $2\phi 22$ to $3\phi 22$. The thickness of the SF concrete layers was $H1 = H2 = 10$ cm and the thickness of the NC layer was $H3 = 10$ cm. The ANSYS numerical simulation analysis shown in Figure 17 took into account non-linear materials.

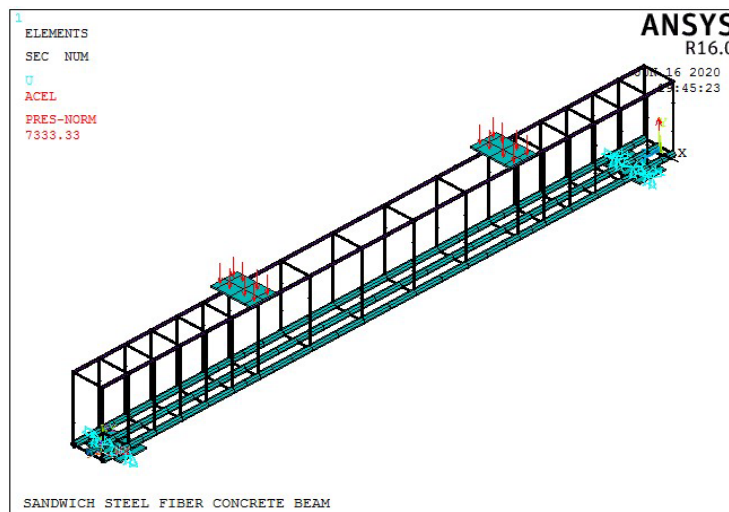
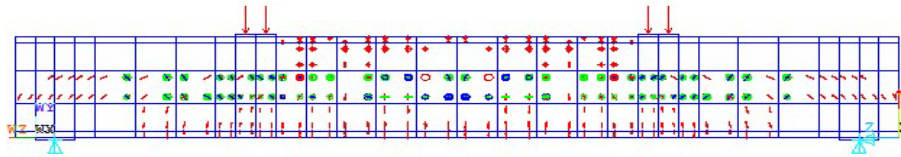


Figure 17. The beam with tensile stress bars number changes.

The beams began to crack and get damaged when the number of TS bar changes, as shown in Figure 18.



a) the beam starts to crack ($P_{crack}=22kN$), $3\phi 22$

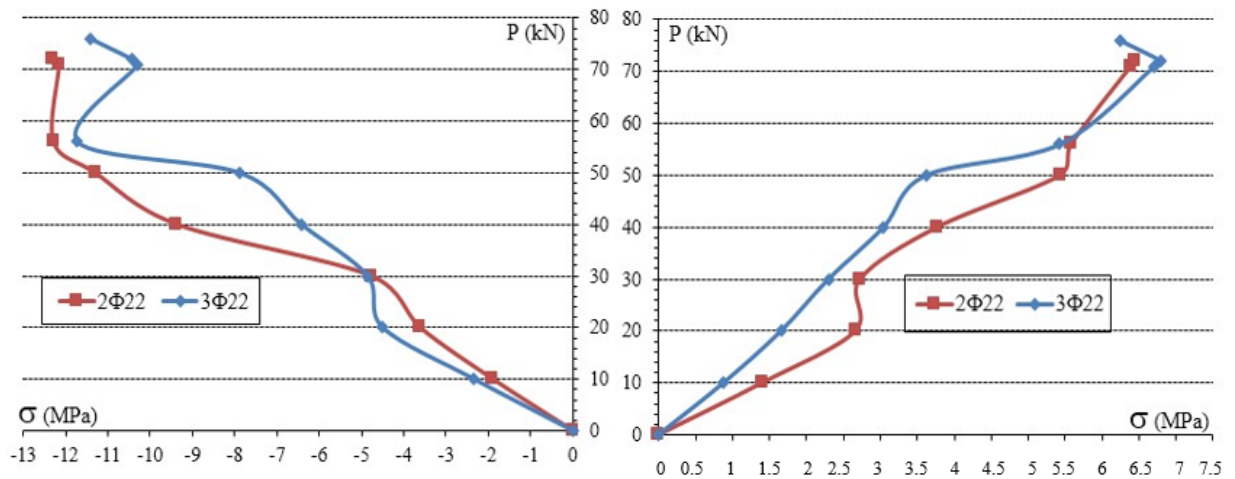


b) the beam starts to fail ($P_{max}=76kN$), $3\phi22$

Figure 18. Beams start to crack and fail when the tensile stress bars number is changed.

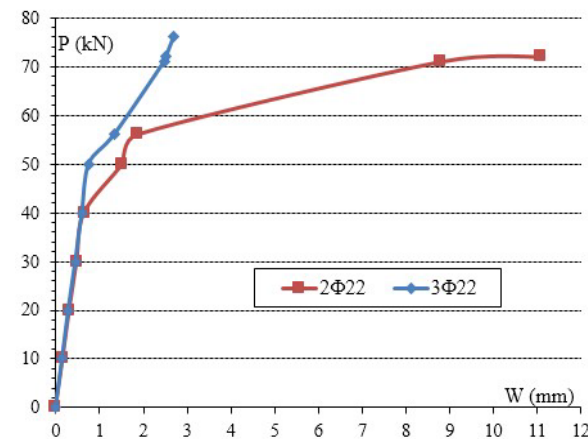
Comment: The beam begin to crack and fail when the number of tensile bars increased to $3\phi22$, compared to when there were only $2\phi22$ tensile bars. The beams in Figure 15a starts to crack at a load of 21 kN. On the other hand, the beams in Figure 18a begin to crack at a load of 22 kN, with an increase of 1 kN afterward. When the beam starts to fail, it occurs at 72 kN for $2\phi22$ beams and at 76 kN for $3\phi22$ beams. However, despite an increase in the TS bars number in the beam, the crack does not show significant changes (as is observed in Figures 8a and 18a). It is worth noting, that the beam only starts to crack in the NC layer located in the middle of the beam.

The L-CS, L-TS and L-VD relationships are shown in Figure 19.



a) load and compressive stress relationship

b) load and tensile stress relationship



c) load and vertical displacement relationship

Figure 19. Load and compressive stress, load and tensile stress and load and vertical displacement relationships.

Comment: In Figure 19a, as the load increases from 0 to 30 kN in compressive stress, the compressive stress between $2\phi22$ and $3\phi22$ remains relatively stable. However, once the load exceeds 30 kN, there is a significant increase in compressive stress, reaching 3 MPa. Tensile stress undergoes a slight change of only 1 MPa in the middle of the beam, as shown in Figure 19b. When the RCB reach a VD of 40 kN, they begin to show changes as the value of $2\phi22$ increases. Additionally, it is worth noting, that

3 ϕ 22 differs significantly from 2 ϕ 22. This demonstrates the effectiveness of increasing the quantity of TS bars in the tensile zone.

3.4. Investigation of the effects of changes in the TS bars diameter

The RCB had a SF content of 2%. The spacing of the stirrups was ϕ 6a100. The TSB consist of 2 ϕ 22, 2 ϕ 16, and 2 ϕ 30 bars. The thickness of the SF concrete layers was H1 = H2 = 10 cm and the thickness of the NC layer was H3=10cm. The ANSYS numerical simulation analysis took into account the nonlinear behavior of the materials.

The beams began to crack and fail when the diameter of the TSB had been changed, as shown in Figure 20.

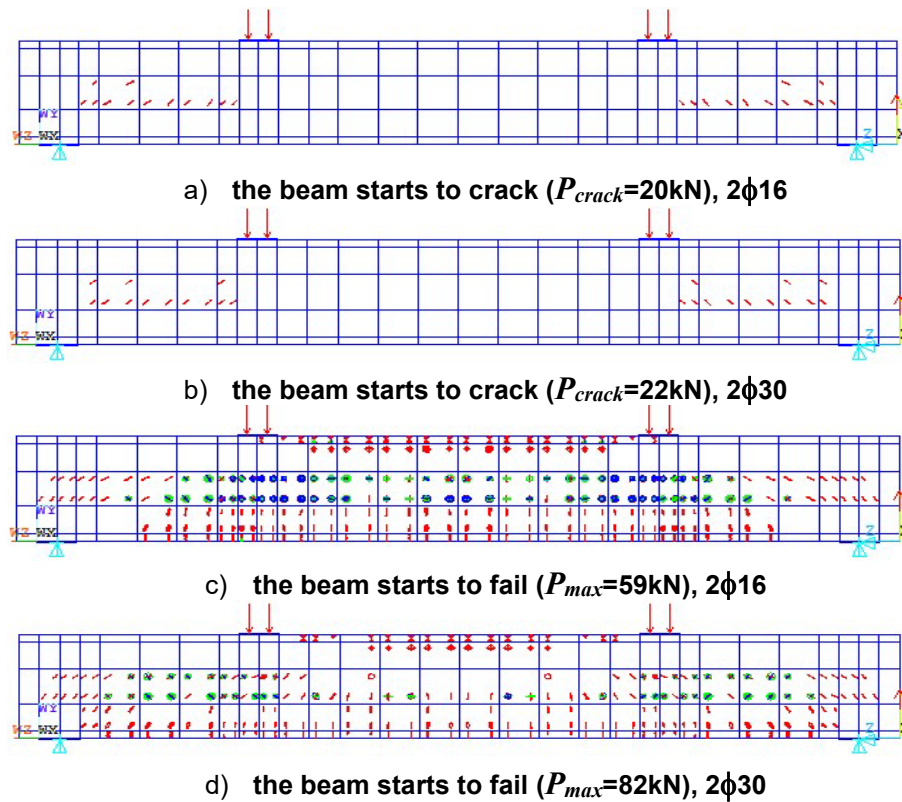
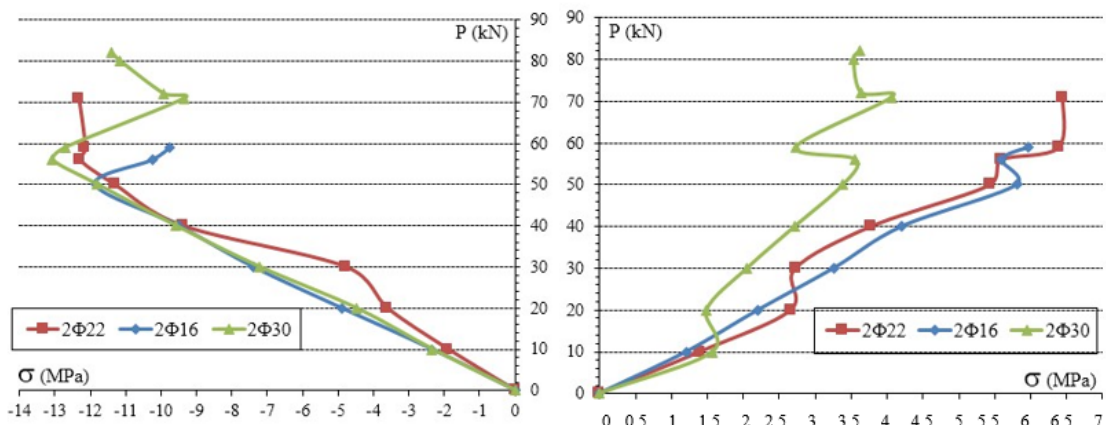


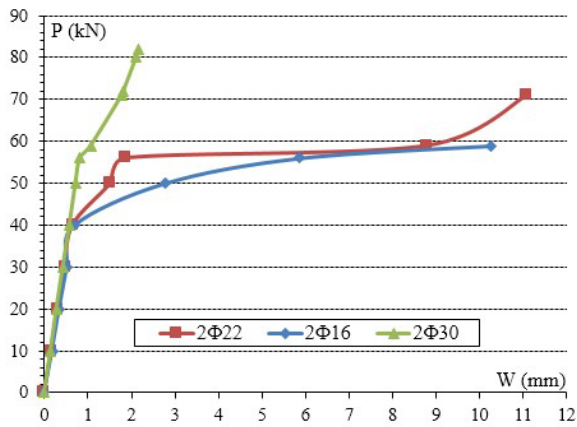
Figure 20. Beams start to crack and fail when diameter of TSB had been changed.

Comment: The cracks in Figures 20a and 20b initially appear in the NC layer. Cracking occurs when the load is applied and the diameter of the TS bar remains relatively unchanged. The limit of the damaged beams varies significantly. Specifically, 2 ϕ 16 beams have a limit of 59 kN, 2 ϕ 22 beams have a limit of 72 kN, and 2 ϕ 30 beams have a limit of 82 kN. The bearing capacity increases to 23 kN between 2 ϕ 16 and 2 ϕ 30, however, there is not a significant change in the number of cracks.

The L-CS, L-TS and L-VD relationships are shown in Figure 21.



a) load and compressive stress relationship b) load and tensile stress relationship



c) load and vertical displacement relationship

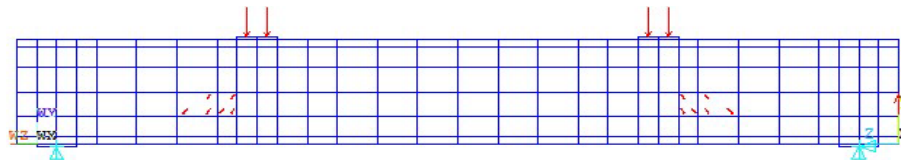
Figure 21. load and compressive stress, load and tensile stress and load and vertical displacement relationships.

Comment: When the diameter of the TS bars is changed, the stresses in the compression zone show minimal changes (as shown in Figure 21a) for the tensile stress of 2Φ16 and 2Φ22. However, for the tensile stress of 2Φ30, there is variation, with a difference of 3 MPa in the tensile stress (as shown in Figure 21b). In the same way, the VD in the beams also varies when the load exceeds 40 kN. During this period, beams of 2Φ16 and 2Φ22 show a higher displacement value compared to beams of 2Φ30.

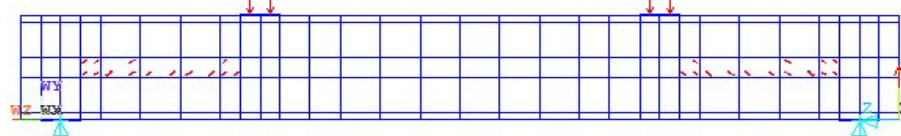
3.5. Investigation of the effect of changes in SF concrete layer that has the same thickness

The RCB had a SF content of 2 %, the spacing of the stirrups was φ6a100. The beam also contained 2Φ22 TS bars and 2Φ10 compression steel bars. The thickness of the concrete layers of SFs was currently H1 = H2 = H = 10 cm, but had been changed to H1 = H2 = H = 8 cm and H1 = H2 = H = 12 cm. The ANSYS numerical simulation analysis took into account the nonlinear behavior of the materials.

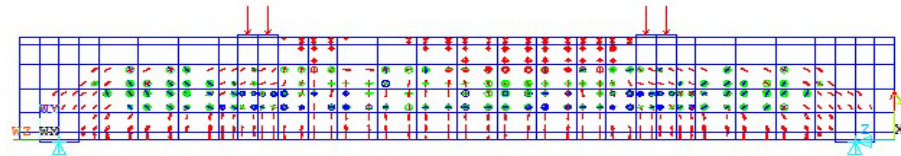
The beams began to crack and fail when there was a change in the thickness of the SF concrete layer, as shown in Figure 22.



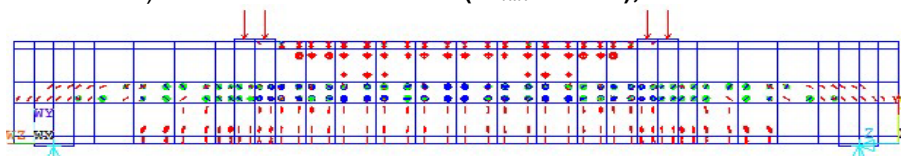
a) the beam starts to crack ($P_{crack}=17kN$), H1=H2=8cm



b) the beam starts to crack ($P_{crack}=21kN$), H1=H2=12cm



c) the beam starts to fail ($P_{max} = 62kN$), H1 = H2 = 8 cm



d) the beam starts to fail ($P_{max}=78kN$), H1=H2=12 cm

Figure 22. Beams start to crack and fail when the thickness of SFCL changes.

Comment: Increasing the thickness of SF concrete layers from 8 to 12 cm results in the improvement of the beam's bearing capacity from 17 to 21 kN. Furthermore, cracks begin to appear in the RCB. In the same way, the bearing capacity of the beams increased from 62 kN to 78 kN during failing. Additionally, there is a significant decrease in the number of cracks observed in the RCB. It is worth noting, that in both cases, the NC layer of the beam showed cracking, as shown in Figure 22.

The L-CS, L-TS and L-VD relationships are shown in Figure 23.

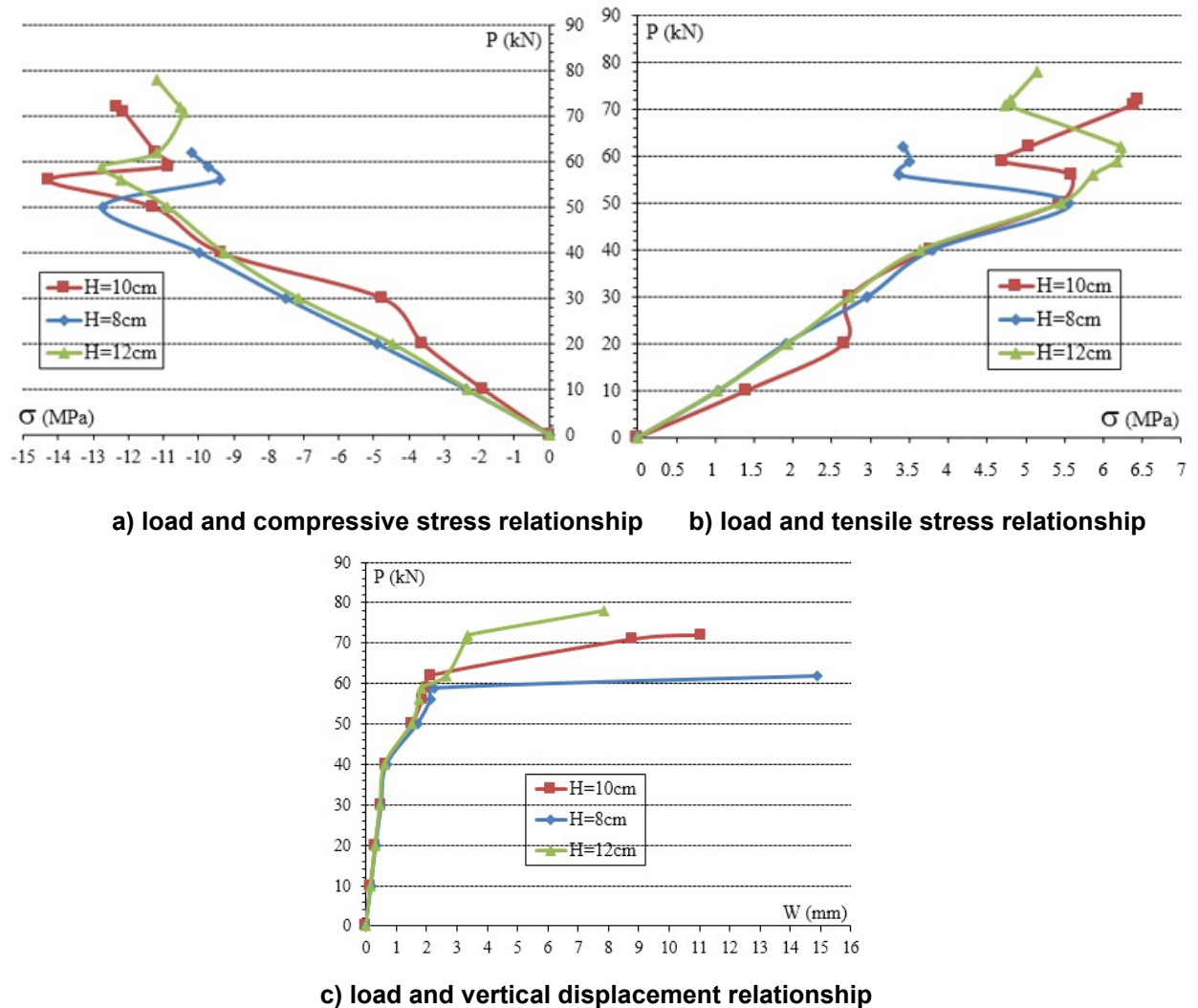


Figure 23. Load and compressive stress, load and tensile stress and load and vertical displacement relationships.

3.6. Comment: In Figure 23, when the thickness of the SF concrete layer is changed without modifying the size of the RCB, the compressive stress, tensile stress and VD in the middle of the beam remain unchanged while the load is varied from 0 kN to 50 kN. The beams undergo a change when the load exceeds this value.

The stresses and VDs of beams with a small thickness of SF concrete layer ($H_1 = H_2 = H = 8$ cm) undergo changes. Investigation of the effects of changes in the thickness of a SF concrete layer

The RCB had a SF content of 2 %. The spacing of the stirrups was $\phi 6a100$. The thickness of the SF concrete layers was $H_1 = H_2 = H = 10$ cm, but it could be changed to $H_1 = 8$ cm and $H_2 = 12$ cm or $H_1 = 12$ cm and $H_2 = 8$ cm. The ANSYS numerical simulation analysis took into account the nonlinear behavior of the materials.

The thickness of the SF concrete layer at the bottom was marked as H_1 , while the thickness of the SF concrete layer at the top was marked as H_2 .

The beams began to crack and fail when there was a change in the thickness of the SF concrete layer, as shown in Figure 24.

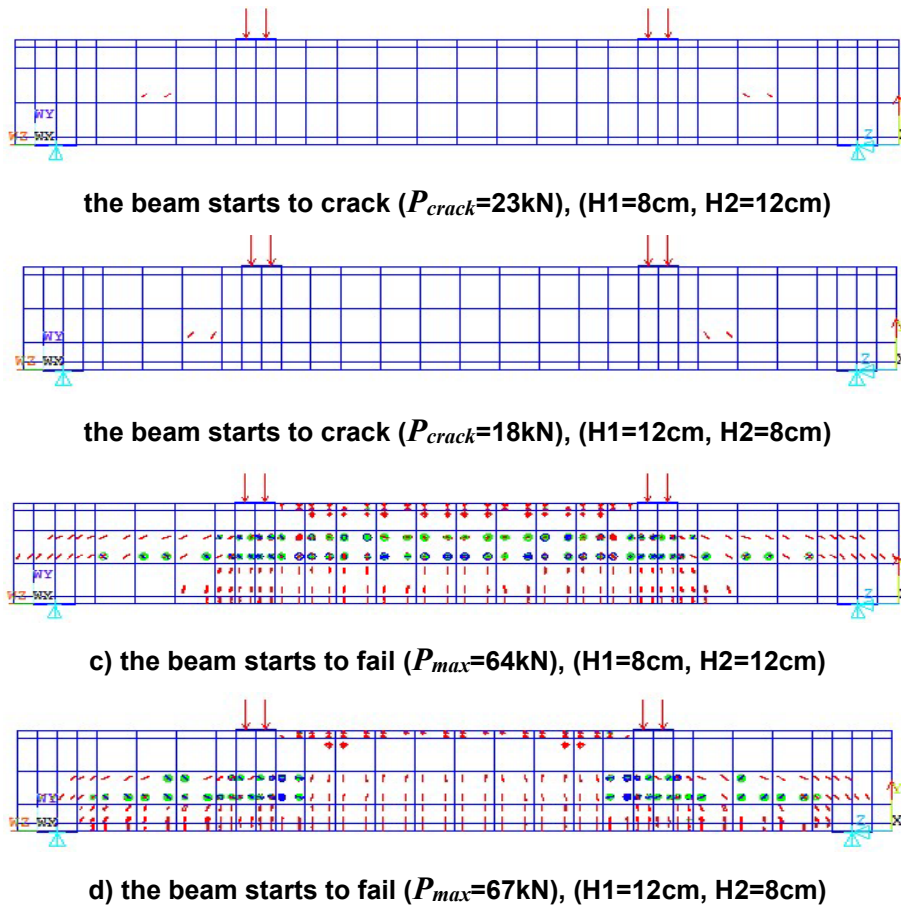
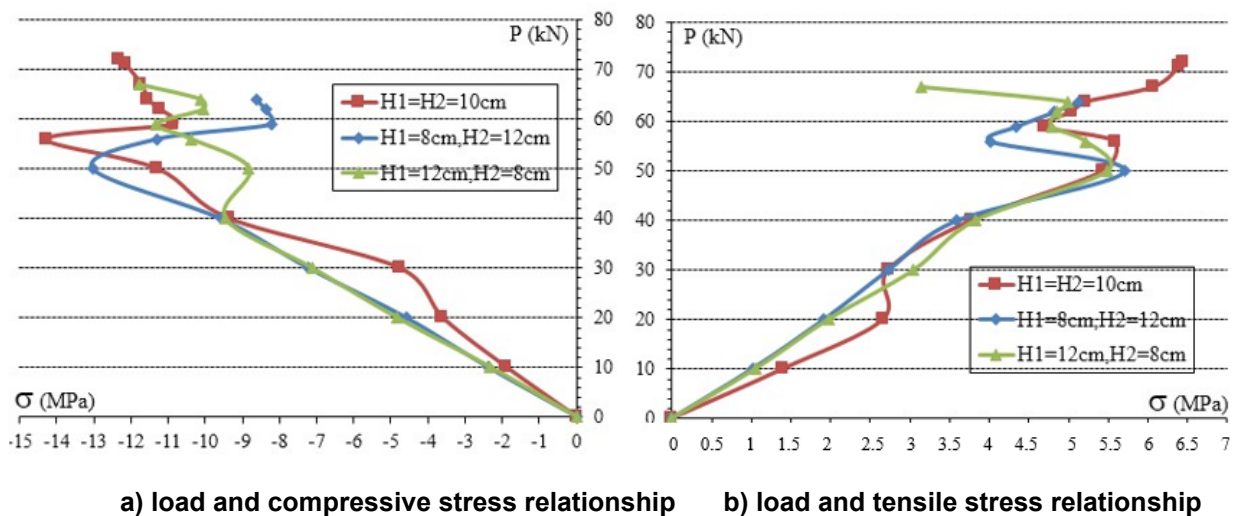
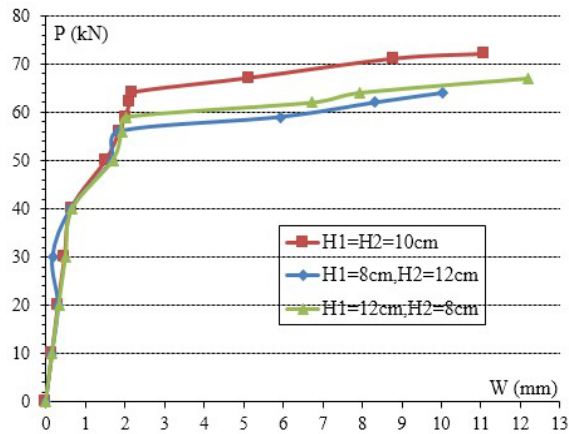


Figure 24. Beams start to crack and fail when thickness of SFCL changes.

Comment: In Figure 24 the top SF concrete layer is thicker than the bottom SF concrete layer. Specifically, the thickness of the top layer (H1) is 8 cm, while the thickness of the bottom layer (H2) is 12 cm. As a result of this configuration, the bearing capacity of the beam increases from 18 kN to 23 kN, when the thicknesses are reversed (H1 = 12 cm, H2 = 8 cm). However, it is important to note that this change in configuration also leads to the formation of cracks in the beam. When the beam is gradually damaged, there is a corresponding change observed. The thickness of the SF concrete layer at the bottom becomes greater than the thickness of the SF concrete layer at the top. This increase in thickness leads to an improvement in bearing capacity, which increases from 64 kN to 67 kN. These findings suggest that increasing the thickness of the SFCL improves its performance.

The L-CS, L-TS and L-VD relationships are shown in Figure 25.





c) load and vertical displacement relationship

Figure 25. Load and compressive stress, load and tensile stress and load and vertical displacement relationships.

Comment: In Figure 25, it can be observed that the change in thickness of various layers of SF concrete does not result in significant changes in the values of compressive stress, tensile stress, and VD. However, it is observed that when the heights of H1 and H2 are both 10 cm, the beam shows a higher bearing capacity compared to other types. This is followed by beams with heights of H1 = 12 cm and H2 = 8 cm, and finally beams with heights of H1 = 8 cm and H2 = 12 cm.

According to this, another experimental study of two-layer RCB [13–14] demonstrates that the cracks observed in the test RCB share similar characteristics in terms of shape, formation, and development of the crack. This is shown in Figures 26 and 27. This study uses ANSYS numerical simulation [18] to investigate crack formation and development in three-layer RCB, as shown in Figure 28.

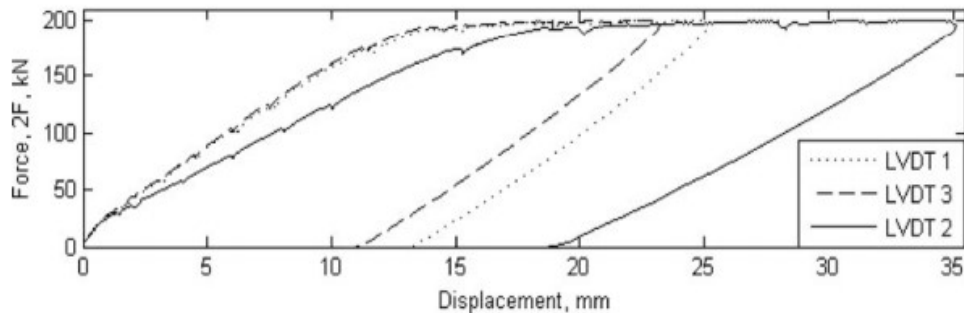


Figure 26. Beam deflections [13].

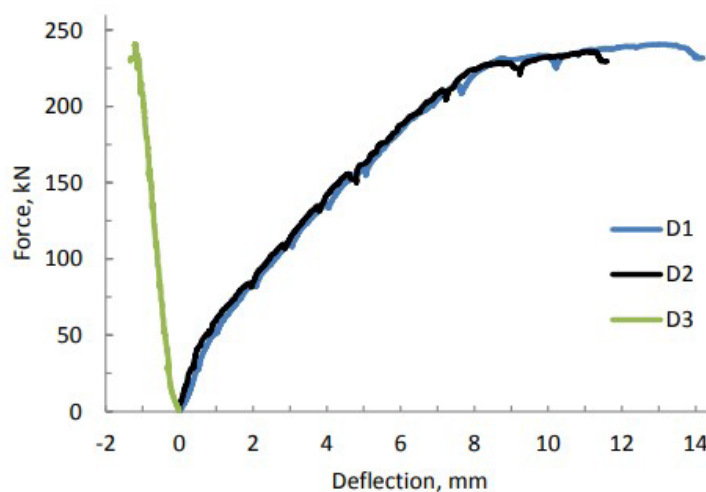


Figure 27. Load Deflection curves in the middle of the spans (D1 and D2) and the mid support uplift (D3) [14].

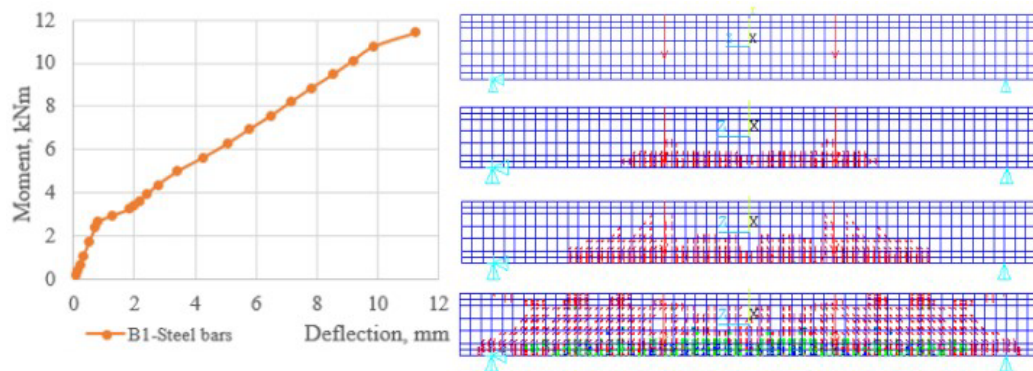


Figure 28. Moment deflection curve and crack pattern [18].

4. Conclusions

Based on the results of the study, we came to the following conclusions:

1. The addition of SFs to concrete resulted in a significant reduction in the number of cracks. When the SF content in the concrete was increased to 4 %, the beam began to experience damage, at a load value that was at least twice as high as the load value for other SF contents.
2. The effectiveness of the beam performance was enhanced by extending the distance between the shear steel bars to 100 mm. The reason for this was that the steel content in the concrete had exceeded the permitted limits.
3. Increasing the number of TS bars and their diameter significantly improved the bearing capacity of the beams, thereby reducing the occurrence of cracks. In this case, the increase in both the number and diameter of the steel bars in the tensile zone had a significant impact on the tensile stress.
4. There was minimal change in the stress value and VD when altering the thickness of the SF concrete layers.
5. The survey conducted on the input parameters of three-layer SF RCB revealed that these parameters had a significant impact on the stress-strain state of the beam. This survey can help modify the parameters needed to restrict or improve specific values that are more appropriate for the design of three-layer SF RCBs.

References

1. Ngo, V.T., Lam, T.Q.K., Do, T.M.D., Nguyen, T.C. Nano concrete aggregation with steel fibers: A problem to enhance the tensile strength of concrete. E3S Web of Conferences. 2019. 135. 03001. DOI: 10.1051/e3sconf/201913503001.
2. Ngo, V.T., Lam, T.Q.K., Do, T.M.D., Nguyen, T.C. Increased plasticity of nano concrete with steel fibers. Magazine of Civil Engineering. 2020. 93(1). Pp. 27–34. DOI: 10.18720/MCE.93.3.
3. Lam, T.Q.K., Do, T.M.D. Stress-strain in multi-layer reinforced concrete doubly curved shell roof. International Journal of Innovative Technology and Exploring Engineering (IJITEE). 2019. 8(4S2). Pp. 419–424.
4. Lam, T.Q.K., Do, T.M.D. Effect of each shell thickness on deformation stress and the ability for causing the cracks in the multilayer doubly curved shell roof. International Journal of Innovative Technology and Exploring Engineering (IJITEE). 2019. 8(6C2). Pp. 215–220.
5. Chepurmenko, A.S. Stress-strain state of three-layered shallow shells under conditions of nonlinear creep. Magazine of Civil Engineering. 2017. 76(8). Pp. 156–168. DOI: 10.18720/MCE.76.14.
6. Lam, T.Q.K., Do, T.M.D., Ngo, V.T., Nguyen, T.C., Huynh, T.P. Numerical simulation and experiment on steel fiber concrete beams. Journal of Physics: Conference Series. 2019. 1425. 012007. DOI: 10.1088/1742-6596/1425/1/012007.
7. Altun, F., Köse, M., Yılmaz, C., Arı, K., Durmuş, A. Experimental investigation of reinforced concrete beams with and without steel fiber under explosive loading. Indian Journal of Engineering & Materials Sciences. 2008. 14. Pp. 419–426.
8. Atlihan, G. Buckling analysis of delaminated composite beams. Indian Journal of Engineering & Materials Sciences. 2013. 20. Pp. 276–282.
9. Soto, A., Tehrani, F.M. An Investigation of Crack Propagation in Steel Fiber-Reinforced Composite Beams. Periodica Polytechnica Civil Engineering. 2018. 62(4). Pp. 956–962. DOI: 10.3311/PPci.10910.
10. Iskhakov, I., Ribakov, Y. A design method for two-layer beams consisting of normal and fibered high strength concrete. Materials & Design. 2007. 28(5). Pp. 1672–1677. DOI: 10.1016/j.matdes.2006.03.017.
11. Travush, V.I., Konin, D.V., Krylov, A.S. Strength of reinforced concrete beams of high-performance concrete and fiber reinforced concrete. Magazine of Civil Engineering. 2018. 77(1). Pp. 90–100. DOI: 10.18720/MCE.77.8.
12. Iskhakov, I., Ribakov, Y. Two-Layer Beams from Normal and Fibered High Strength Concrete. Conference: Modern Methods and Advances in Structural Engineering and Construction. 2011. DOI: 10.3850/978-981-08-7920-4_S3-M029-cd.
13. Iskhakov, I., Ribakov, Y., Holschemacher, K., Mueller, T. Experimental Investigation of Full Scale Two-Layer Reinforced Concrete Beams. Mechanics of Advanced Materials and Structures. 2014. 21. Pp. 273–283. DOI: 10.1080/15376494.2012.680673.

14. Iskhakov, I., Ribakov, Y., Holschemacher, K. Experimental investigation of continuous two-layer reinforced concrete beams. *Structural Concrete*. 2017. 18(1). Pp. 205–215. DOI: 10.1002/suco.201600027.
15. Iskhakov, I., Ribakov, Y., Holschemacher, K., Kaeseberg, S. Experimental investigation of prestressed two layer reinforced concrete beams. *Structural Concrete*. 2021. 22(1). Pp. 238–249. DOI: 10.1002/suco.201900328.
16. Pratama M.M.A., Suhud, R.K., Puspitasari, P., Kusuma, F.I., Putra, A.B.N.R. Finite element analysis of the bending moment-curvature of the double-layered graded concrete beam. *IOP Conf. Series: Materials Science and Engineering*. 2019. 494. 012064. DOI: 10.1088/1757-899X/494/1/012064.
17. Vu, D.T., Korol, E.A. Influence of geometrical parameters of the cross section, strength and deformability of the materials used on stress-strain state of three-layered reinforced concrete. *IOP Conf. Series: Materials Science and Engineering*. 2019. 661. 012121. DOI: 10.1088/1757-899X/661/1/012121.
18. Vu, D.T., Korol, E., Kustikova, Yu., Nguyen, H.H. Finite element analysis of three-layer concrete beam with composite reinforcement. *E3S Web of Conferences*. 2019. 97 02023. DOI: 10.1051/e3sconf/20199702023.
19. Do, T.M.D., Lam, T.Q.K. Design parameters of steel fiber concrete beams. *Magazine of Civil Engineering*. 2021. 102(2). 10207. DOI: 10.34910/MCE.102.7.
20. Olmedo, F.I., Valivonis, J., Cobo, A. Experimental study of multilayer beams of lightweight concrete and normal concrete. *Procedia Engineering*. 2017. 172. Pp. 808–815. DOI: 10.1016/j.proeng.2017.02.128.
21. Ranjbaran, F., Rezayfar, O., Mirzababai, R. Experimental investigation of steel fiber-reinforced concrete beams under cyclic loading. *International Journal of Advanced Structural Engineering*. 2018. 10. Pp. 49–60. DOI: 10.1007/s40091-018-0177-1.
22. Muselemov, Kh.M., Bulgakov, A.I., Muselemov, Dz.U. Stress-Strain State of an Unsymmetrical Three-Layer Beam. *Modern Trends in Construction, Urban and Territorial Planning*. 2023. 2(4). Pp. 27–33. DOI: 10.23947/2949-1835-2023-2-4-27-33.
23. Do, T.M.D., Lam, T.Q.K. Cracks in single-layer and multi-layer concrete beams. *Transportation Research Procedia*. 2022. 63. Pp. 2589–2600. DOI: 10.1016/j.trpro.2022.06.298.
24. Su, C., Liu, D., Cao, S., et al. Analysis of static and dynamic flexural and tensile failure modes of double-layer concrete composite beams [J]. *Journal of Southwest Jiaotong University*. 2017. 52(4). Pp. 731–737. DOI: 10.3969/j.issn.0258-2724.2017.04.011.
25. Najm, H.B. Flexural Behavior of Two-layers Reinforced Concrete Beams. *Polytechnic Journal*. 2022. 12(2). Pp. 180-192. DOI: 10.25156/ptj.v12n2y2022.pp180-192.
26. TrustGod, J.A., Blessing, B.T. Optimum Depth of a Lower Concrete Grade at the Tension Zone in a Two-Layer Reinforced Concrete Beam. *Nigerian Journal of Technological Development*. 2023. 20(1). Pp. 1–8. DOI: 10.4314/njtd.v20i1.1197.

Information about author:

Thanh Quang Khai Lam, PhD

ORCID: <https://orcid.org/0000-0003-3142-428X>

Email: lamthanhquangkhai@gmail.com

Received 01.08.2020. Approved after reviewing 08.10.2021. Accepted 09.10.2023.